Published in final edited form as:
Cell Metab. 2013 June 4; 17(6): 916–928. doi:10.1016/j.cmet.2013.04.007.

Diet1 functions in the FGF15/19 enterohepatic signaling axis to modulate bile acid and lipid levels

Laurent Vergnes[1,*], **Jessica M. Lee**[1,*], **Robert G. Chin**[1], **Johan Auwerx**[2], and **Karen Reue**[1,3]

[1]Department of Human Genetics, David Geffen School of Medicine at UCLA [2]Ecole Polytechnique Fédérale de Lausanne, Lausanne, Switzerland [3]Molecular Biology Institute, University of California, Los Angeles

Abstract

We identified a mutation in the *Diet1* gene in a mouse strain that is resistant to hyperlipidemia and atherosclerosis. *Diet1* encodes a 236 kD protein consisting of tandem low density lipoprotein receptor and MAM (meprin-A5-protein tyrosine phosphatase mu) domains, and is expressed in enterocytes of the small intestine. Diet1-deficient mice exhibited an elevated bile acid pool size and impaired feedback regulation of hepatic *Cyp7a1*, which encodes the rate-limiting enzyme in bile acid synthesis. In mouse intestine and in cultured human intestinal cells, *Diet1* expression levels influenced the production of fibroblast growth factor 15/19 (FGF15/19), a hormone that signals from the intestine to liver to regulate *Cyp7a1*. Transgenic expression of *Diet1*, or adenoviral-mediated *Fgf15* expression, restored normal *Cyp7a1* regulation in Diet-1–deficient mice. Diet1 and FGF19 proteins exhibited overlapping subcellular localization in cultured intestinal cells. These results establish Diet1 as a control point in enterohepatic bile acid signaling and lipid homeostasis.

Introduction

Impaired regulation of bile acid production and cholesterol excretion are underlying factors in the pathogenesis of several common clinical conditions such as hypercholesterolemia, cardiovascular disease, bile acid malabsorption, gallstone disease, and type 2 diabetes (Angelin et al., 1999; Goldfine, 2008; Hageman et al., 2010; Khurana et al., 2011; Thomas et al., 2008; Walters and Pattni, 2010). Bile acids are synthesized from cholesterol in the liver in a highly regulated manner, stored in the gall bladder, and secreted into the duodenum in response to a meal (Hofmann, 2009; Hylemon et al., 2009; Lefebvre et al., 2009; Russell, 2003, 2009). Bile acids play a critical role in the absorption of dietary fats and fat-soluble vitamins in the upper small intestine, prior to reabsorption of approximately 95% of bile acids in the ileum. The remaining 5% of bile acids are excreted, providing a means for sterol elimination from the body. Prior to the availability of statin drugs for the treatment of hypercholesterolemia, the use of bile acid sequestrants was a common strategy to lower cholesterol levels (Angelin et al., 1999). Bile acid sequestration leads to reduced bile acid reabsorption, increased conversion of cholesterol to bile acids in the liver,

Correspondence: Karen Reue, Department of Human Genetics, David Geffen School of Medicine at UCLA, Gonda Center 6506A, 695 Charles E. Young Drive South, Los Angeles, CA 90095. Tel (310) 794-5631, Fax (310) 794-5446, reuek@ucla.edu.
*These authors contributed equally to this work.

Conflict of Interest: The authors declare no conflict of interest.

Author contributions: K.R. and L.V. designed research; L.V., J.M.L., and R.G.C. performed research; J.A. contributed analytic tools; K.R. wrote the paper.

increased LDL receptor expression, and reduced lipoprotein cholesterol levels. In recent years, bile acid sequestrants have reemerged as a potential treatment paradigm for conditions ranging from bile acid malabsorption to type 2 diabetes (Aggarwal et al., 2012; Goldfine, 2008; Handelsman, 2011; Thomas et al., 2008; Westergaard, 2007).

Also in recent years there has been a leap forward in our understanding of the regulation of bile acid homeostasis. An intricate mechanism exists for feedback regulation of bile acid synthesis involving communication from the small intestine to the liver via fibroblast growth factor 15 (FGF15) in mouse, or FGF19 in humans (reviewed in Cicione et al., 2012; Jones, 2012; Potthoff et al., 2011). In the small intestine, bile acids activate the farnesoid X receptor (FXR) to promote *Fgf15/FGF19* gene transcription and protein secretion into the enterohepatic circulation. Upon reaching the liver, FGF15/19 interacts with the FGF receptor 4/β-klotho complex, and leads to transcriptional repression of the *Cyp7a1* gene, which encodes the rate-limiting enzyme for the classic pathway of bile acid synthesis (Inagaki et al., 2005; Kim et al., 2007; Lundasen et al., 2006). A recent study has shown that conditions characterized by bile acid malabsorption in humans are often associated with decreased FGF19 levels, suggesting that increased bile acid synthesis, rather than impaired absorption, is the likely culprit (Walters et al., 2009). Thus, an understanding of factors that regulate FGF15/19 levels is of interest. In addition to FXR, vitamins A and D regulate *Fgf15* gene transcription through the action vitamin D and retinoid–responsive nuclear receptors (Schmidt et al., 2010). It is unknown whether additional control points for FGF15/19 production operate.

Several years ago, Lusis and colleagues identified a sub-strain of C57BL/6 mice, C57BL/6ByJ, which had low circulating lipid levels and resistance to atherosclerosis (Mouzeyan et al., 2000). This was notable because the C57BL/6J mouse strain from which the sub-strain was derived is highly susceptible to hypercholesterolemia and atherosclerosis. We found that the resistance to hypercholesterolemia in C57BL/6ByJ mice was associated with increased bile acid excretion in the feces (2-fold) and urine (18-fold) (Phan et al., 2002). In a genetic cross, the reduced plasma cholesterol levels and elevated bile acid levels co-segregated, indicating that a single genetic locus was responsible for controlling both (Phan et al., 2002). We hypothesized that a mutation had occurred in C57BL/6ByJ mice that led to dysregulated bile acid metabolism. Here we report the identification of the responsible mutation in a previously uncharacterized gene, *Diet1*, and demonstrate that Diet1 has a role in the FGF15/19 intestine-liver axis for the regulation of bile acid synthesis.

Results

Identification of the *Diet1* gene and null mutation in C57BL/6ByJ (B6By) mice

The *Diet1* locus was previously mapped to a 20 cM region on proximal chromosome 2 (Mouzeyan et al., 2000). To map the gene to high resolution, we generated a backcross between B6By and CAST/EiJ mice, and typed bile acid levels in 790 offspring to narrow the *Diet1* locus to a region of approximately 11 Mb, between markers *D2Mit359* and *D2Mit6*. Mice that were homozygous for the B6By allele throughout this region exhibited high serum bile acid levels (>30 μM), whereas heterozygous mice exhibited low bile acid levels (<10 μM). Mice with recombination events within this interval were used to further narrow the *Diet1* locus. To confirm correspondence between bile acid levels and genotype, recombinant mice were subjected to progeny testing by backcrossing to B6By mice. At least 20 backcross offspring from each recombinant were subsequently typed for bile acid levels and genetic markers. This analysis narrowed the *Diet1* mutation to a 2.4 Mb region between *D2Mit360* and *D2Mit267* (Figure 1A; Table S1), which harbors four known genes and a few small predicted genes, which we later found comprise a single novel gene (see below).

The four known genes in the *Diet1* gene critical interval showed normal mRNA expression levels in B6By mouse tissues (Figure S1). However, analysis of the novel predicted gene sequence showed prominent expression of a 7 kb mRNA in the small intestine of control C57BL/6J (B6J) mice that was absent in B6By mice fed either chow or atherogenic diets (Figure 1B). We used a combination of genome sequence information and 5' and 3' RACE (rapid amplification of cDNA ends) to isolate a full-length 6963 bp cDNA from B6J intestinal RNA. Mapping the cDNA sequence to the mouse genome revealed that the *Diet1* gene spans approximately 730 kb and comprises 39 exons (Figure 1D, top line). To identify the mutation present in the B6By genome, we sequenced each of the 39 exons and all intron/exon junctions, but found no differences in B6By compared to the wild-type B6J. However, using portions of the *Diet1* cDNA to probe genomic Southern blots, we found that a probe corresponding to exon 23 of the *Diet1* gene produced an abnormal hybridization pattern with B6By DNA (Figure 1C). Extra bands were detected in digests with different restriction enzymes, suggesting that duplication of a portion of the *Diet1* gene has occurred in the B6By genome. Sequence analysis revealed that the B6By genome contains a duplication of exons 21, 22, and 23 (Figure 1D). The inclusion of these inserted exons in the *Diet1* mRNA transcript introduces a frame-shift and premature stop codon (Figure 1D, lower line), presumably resulting in nonsense-mediated mRNA decay and accounting for the absence of detectable *Diet1* mRNA by Northern blot (Figure 1B).

Diet1 is an evolutionarily conserved modular protein

Mouse *Diet1* encodes a protein of 2123 amino acids and predicted molecular weight of 236 kD. Analysis of the protein sequence revealed several known protein domains (Figure 1E). Accounting for a large portion of the protein are 9 copies of the MAM (meprin-A5-protein tyrosine phosphatase mu) domain, a 170 amino acid domain that contains 4 conserved cysteine residues that likely form two disulfide bridges (Beckmann and Bork, 1993). The MAM domain is a component of numerous proteins with diverse functions, and has been implicated in protein-protein interactions, signal transduction, and cell-cell adhesion (Cismasiu et al., 2004; Ishmael et al., 2005). Also present in Diet1 are 9 low density lipoprotein receptor (class A) domains, an epidermal growth factor-like (subtype 2) domain, and a putative transmembrane domain near the C-terminus (Figure 1E). LDL receptor domains are approximately 40 amino acids in length, contain six disulfide-bound cysteines and a highly conserved cluster of negatively charged amino acids, which affect LDL receptor binding to its apolipoprotein ligands (Yamamoto and Ryan, 2009).

We sequenced *Diet1* cDNA from intestinal mRNA of additional species, including human, rat, chicken, frog and zebrafish. The predicted Diet1 protein sequences are highly conserved with a nearly identical MAM-LDL receptor domain organization (Figure 1E). The human *DIET1* gene spans 686 kb on chromosome 10p12 and encodes a predicted protein of 2156 amino acids that is 70% identical to mouse Diet1. Based on both the experimentally determined cDNA and genomic DNA sequences, the zebrafish protein appears to be truncated at the amino-terminal end relative to the other species. We could not identify *Diet1* orthologs in invertebrates or lower organisms. Of known proteins, Diet1 had significant similarity to endotubin (also known as apical early endosomal glycoprotein), a 140 kD membrane glycoprotein containing 5 MAM and 2 LDL receptor domains (Allen et al., 1998; Gokay et al., 2001; Wilson and Colton, 1997). Endotubin regulates trafficking of tight junction proteins in polarized epithelial cells (McCarter et al., 2010).

Diet1 is expressed in intestinal epithelial cells

To begin to understand its physiological function, we characterized the tissue distribution and developmental profile of *Diet1* expression. *In situ* hybridization to cross-sections through an adult mouse indicated that *Diet1* expression is limited to the small intestine and

kidney cortex, and is not detected in other tissues including liver (Figure 2A). *In situ* hybridization of mouse embryos failed to detect expression during mid-gestation (at 9.5, 12.5, and 14.5 dpc), but detected *Diet1* mRNA in the intestinal primordium at 15.5 dpc, and increasing expression levels through postnatal days 1 and 10, attaining a maximal level in adulthood (Figure S2). Gene expression analysis by RT-PCR in tissue panels from mouse (Figure 2B) and human (Figure 2C) confirmed that *Diet1* is expressed predominantly in the small intestine, with low level expression also detected in mouse kidney and testis. In mouse intestine, *Diet1* mRNA levels increased along the length of the small intestine from duodenum to ileum, and were not detected in stomach or colon (Figure 2D and S3). High resolution *in situ* hybridization revealed that *Diet1* expression was localized to the villi in the intestinal lumen, and the signal was present in the epithelial cell layer, but not in the lamina propria, smooth muscle layer or serosa (Figure 2E and S3).

To assess whether *Diet1* expression is regulated during intestinal epithelial cell development, we utilized the human Caco-2 cell line, which differentiates *in vitro* to acquire properties of small intestine epithelial cells, including expression of the brush border microvilli and enzymes, formation of tight junctions, and a variety of transport functions (Rousset et al., 1985). *DIET1* mRNA expression was very low in undifferentiated cells, and was induced 120-fold during Caco-2 cell differentiation, in concert with the expression of sucrose isomaltase (Figure 2F). These observations suggest that Diet1 functions primarily in mature intestinal epithelial cells.

To investigate the subcellular localization of Diet1 protein, we performed immunofluorescence confocal microscopy on mouse ileum sections. To ensure specific detection of Diet1 without cross-reactivity to other endogenous proteins, we generated C57BL/6J mice expressing a *Diet1* cDNA with a carboxyl-terminal V5 epitope tag under control of the ileal fatty acid binding protein (IFABP) regulatory elements (Cohn et al., 1992). As dictated by the IFABP promoter, Diet1-V5 protein was expressed in enterocytes lining the villi. Diet1-V5 protein appeared in a punctate distribution within the cytosol and was not present in the apical enterocyte membrane, as determined by lack of co-localization with the ileal apical sodium-dependent bile acid transporter (ASBT, also known as Slc10a2) (Figure 2G,H). These observations suggest that the predicted membrane-spanning region of the protein is associated with the membrane of an intracellular compartment, although we cannot rule out the possibility that Diet1 transiently cycles to the cell membrane.

Diet1 deficiency reduces ileal FGF15 levels and impairs the regulation of hepatic bile acid metabolism genes

We previously observed that B6By mice exhibit elevated plasma bile acid levels and enhanced bile acid excretion compared to C57BL/6J mice (Phan et al., 2002). Analysis of bile acids in blood and tissues by gas chromatography/mass spectrometry revealed an expanded bile acid pool size in B6By mice in the circulation, liver, and gastrointestinal tract (duodenum, jejunum, ileum, gall bladder) (Figure 3A). Elevations were observed across bile acid species, with the most notable increase occurring in cholic acid levels, in the form of tauro-conjugated bile acids (Figure 3B).

Consistent with the increased bile acid pool size, B6By mice had elevated expression of genes involved in bile acid synthesis in the liver, including *Cyp7a1* and *Cyp27* (Figure 3C and Phan et al., 2002). We also detected enhanced hepatic expression of genes for the bile salt export pump (*Abcb11*) and the liver receptor homolog-1 nuclear receptor (*Nr5a2*), which modulates *Cyp7a1* expression levels (Figure 3C).

Since *Diet1* expression is not detectable in liver (Figure 2), it was unclear how Diet1 deficiency influences hepatic gene expression and bile acid levels. One possibility was that

Diet1-deficient mice have reduced bile acid uptake in the ileum leading to increased bile acid excretion and a compensatory increase in bile acid production in the liver. Bile acid uptake in the ileum is governed by ASBT, encoded by *Slc10a2* (Dawson et al., 2009). Both mRNA levels and protein levels for ASBT were normal or elevated in B6By compared to C57BL/6J mice (Figure 3D, E). Furthermore, ASBT protein was visible on the apical membrane of ileum in B6By mice (Figure 3F, G). Thus, the elevated bile acid levels in B6By mice appear not to result from defective ASBT production or localization.

We searched for another mechanism that could explain the elevated bile acid levels and the persistence of high bile acid biosynthetic gene expression in liver of Diet1-deficient mice. B6By mice had normal intestinal mRNA levels for the Ostα and Ostβ bile acid transporters located on the basolateral surface of the enterocytes, intestinal bile acid binding protein (*Fabp6*), nuclear receptors FXRα (*Nr1h4*), LXRα (*Nr1h3*), and the short heterodimeric partner (*Nr0b2*) (Figure 3D). However, we detected significantly reduced mRNA levels for fibroblast growth factor 15 (*Fgf15*) (Figure 3D), a hormone that is synthesized in the ileum and signals through the enterohepatic circulation to down-regulate *Cyp7a1* expression in the liver (Inagaki et al., 2005; Jones, 2008). FGF15 protein levels in the ileum of B6By mice were also decreased compared to C57BL/6J mice (Figure 3H). The expression of fibroblast growth factor receptor 4 (*Fgfr4*), a co-receptor for FGF15 on the hepatocyte surface, was elevated 2-fold in B6By liver (Figure 3C), suggesting that B6By liver is primed to respond to FGF15. Based on our results, we hypothesized that Diet1 influences FGF15 production in the intestine, leading to downstream effects on the regulation of hepatic *Cyp7a1* expression.

Diet1 levels influence *Fgf15* and *Cyp7a1* expression *in vivo*

To test our hypothesis, we assessed whether increasing the levels of Diet1 *in vivo* leads to enhanced *Fgf15* expression and reduced *Cyp7a1* expression. As described above, we generated C57BL/6J mice that express a *Diet1*-V5 transgene in small intestine. Transgene expression was detectable in intestine using qPCR with transgene-specific PCR primers (Figure S4A). However, the transgene expression levels were low compared to endogenous *Diet1* expression levels, and therefore did not significantly increase the total levels of *Diet1* mRNA in the wild-type C57BL/6J strain background (Figure S4A). Therefore, we could not use this mouse model to assess the consequences of *Diet1* overexpression. However, the *Diet1* transgenic strain was valuable for complementation of Diet1 deficiency in B6By mice.

Introduction of the *Diet1* transgene into the B6By strain increased *Diet1* mRNA expression to detectable levels (Figure 4A). The *Diet1* transgene expression levels differed between sexes, with female transgenics (Figure 4A) expressing higher *Diet1* mRNA levels than males (Figure S4B). Compared to B6By mice, B6By + Diet1 Tg mice had significantly higher *Fgf15* mRNA levels, and a trend to reduced *Cyp7a1* mRNA levels (Figure 4A and S4B). An analysis of expression levels in all of the male and female mice revealed highly significant positive correlations between *Diet1* and *Fgf15* expression levels, and inverse correlations between *Diet1* and *Cyp7a1*, and *Fgf15* and *Cyp7a1* expression levels (Figure 4B). Thus, changes in *Diet1* expression levels lead to correlative increases in *Fgf15* mRNA levels, and inverse effects on *Cyp7a1* expression levels.

As further evidence that the impaired feedback regulation of *Cyp7a1* in Diet1-deficient mice results from reduced FGF15 levels, we restored FGF15 expression in B6By mice by adenovirus-mediated FGF15 expression. Mice were administered recombinant adenovirus expressing FGF15 (Inagaki et al., 2005) or lacZ, and tissues collected 6 days later. Infection with FGF15-expressing adenovirus dramatically reduced *Cyp7a1* expression in B6By mouse liver (Figure 4C). In addition to bile acid synthesis, FGF15 inhibits hepatic glucose production (Potthoff et al., 2011). Consistent with this, administration of FGF15 also reduced the fasting glucose levels observed in B6By mice, and this was reflected in reduced

expression of glucose-6 phosphatase (Figure 4C). These findings indicate that the defect in bile acid feedback regulation in B6By mice is reduced availability of FGF15, and that the signaling pathway downstream of FGF15 is not impaired in B6By mice.

Diet1 modulates levels of FGF19 secreted from cultured intestinal cells

To investigate whether Diet1 levels acutely influence FGF15 production in intestinal cells, we modulated Diet1 levels in cultured intestinal cells. The most well-established intestinal cell lines are of human origin, and we screened three cell lines for expression and secretion of FGF19, the human ortholog of mouse FGF15. Of three human intestinal cell lines (HT-29, Caco-2, COLO 205) (Semple et al., 1978; Zweibaum et al., 1983), HT-29 cells expressed and secreted FGF19 most robustly, and we therefore selected these cells for our studies. We investigated whether acute alterations in *Diet1* expression levels influence levels of FGF19 mRNA expression and FGF19 protein secreted into the medium. HT-29 cells transfected with a *Diet1* expression vector increased FGF19 mRNA levels slightly (~30%), and increased FGF19 protein secretion into the culture medium by 3-fold (left panels in Figure 5A, B, C). In the complementary experiment, a 60% knockdown in *Diet1* mRNA levels did not affect FGF19 mRNA expression, but reduced FGF19 levels in the culture medium by 30% (right panels in Figure 5A, B, C). The secretion of apolipoprotein A–I was not affected by modulating Diet1 levels (Figure 5D), indicating that the effects on FGF19 results are not due to a non-specific effect on secreted proteins.

Our results indicated that Diet1 has a modest effect on FGF19 mRNA levels and a pronounced effect on FGF19 protein levels, but did not distinguish whether the protein levels increase secondary to mRNA levels, or are also influenced by Diet1 at the post-transcriptional level. To investigate whether Diet1 influences FGF19 protein levels in a transcription-independent manner, we expressed FGF19 under the control of a heterologous promoter that is transcribed at a constitutive level. Increasing amounts of Diet1 led to increased levels of cellular and secreted FGF19 protein (Figure 5E, F). These results indicate that Diet1 has an effect on FGF19 protein production that is independent of an effect on FGF19 mRNA levels. Taken together, our results from *in vivo* and *in vitro* systems indicate that Diet1 influences FGF15/FGF19 levels at both the mRNA and post-transcriptional levels.

Diet1 co-localizes with and interacts with FGF15

As described above, Diet1 influences FGF19 levels, in part, through a post-transcriptional mechanism. To further characterize the relationship between Diet1 and FGF15 proteins, we examined their subcellular localization in intestinal cells. For these studies we used the IEC-6 rat intestinal cell line (Quaroni et al., 1979) because it allows better visualization of proteins in the cytoplasm than human cell lines that we tested (Caco-2, HT-29 or COLO 205). As we observed in mouse intestine (Figure 2G), Diet1 was present in a punctate cytosolic pattern (Figure 6A). FGF15 also appeared in a punctate cytosolic distribution, and there appeared to be substantial overlap between Diet1 and FGF15 (yellow signal in Figure 6A and 6B). A proportion of Diet1 and FGF15 co-localized in structures having a vesicle-like appearance (Figure 6B, arrowheads). This suggested that Diet1 might be present in an endosomal / lysosomal trafficking compartment, and we sought to co-localize Diet1 with established vesicular trafficking markers. We could not detect any co-localization of Diet1 with markers of early endosomes (EEA1 and Rab5), late endosomes (Rab7), or lysosomes (LimpII) (Figure 6C). Thus, Diet1 and FGF15 may reside in a distinct vesicular subtype.

The close proximity of Diet1 and FGF15 within the cell raised the possibility that the two proteins physically interact. Immunoprecipitation directly from mouse intestine was not possible as our antibodies detected several non-specific bands in this tissue (not shown). We

therefore expressed human Diet1-V5 and FGF19-Myc tagged proteins in human HEK293 cells and assessed whether the two proteins co-immunoprecipitated. When expressed in combination, human Diet1 and FGF19 co-immunoprecipitated, as did mouse Diet1 and FGF15 (Figure 6D, top panels, starred bands). The conservation of this interaction with both human and mouse proteins is significant given that the FGF19 and FGF15 diverge substantially in their primary amino acid sequence (approximately 50% identity) (Wright et al., 2004). Precipitations were specific, as shown by lack of precipitation with IgG or with unrelated proteins carrying the same epitope tags (Kdm5c-V5 and FABP6-Myc) (Figure 6D, control panels). The direct effect of Diet1 on FGF19 protein (Fig. 5E, F), and the subcellular co-localization and protein-protein interactions between Diet1 and FGF15/19, suggest that impairment of this interaction in Diet1 deficiency contributes to the reduced FGF15/19 levels observed.

Discussion

Spontaneous mutations in mice and humans have been valuable tools for the discovery of critical protein functions in metabolism. We capitalized on a spontaneous mutation that occurred in the C57BL/6ByJ mouse strain to identify *Diet1*. We previously determined that B6By mice have elevated bile acid levels and substantial bile acid excretion in the urine and feces (Phan et al., 2002). They also have reduced plasma lipid levels compared to C57BL/6J mice, and we proposed that the enhanced conversion of cholesterol to bile acids, followed by excretion constitutes a means for reducing circulating cholesterol levels (Mouzeyan et al., 2000; Phan et al., 2002). However, without knowing the genetic lesion underlying this phenotype, we were unable to determine the physiological mechanism for the increased bile acid synthesis. Here we demonstrate that B6By mice carry a null mutation in a previously unknown gene, *Diet1*. Diet1 has a role in the FGF15/19 axis that serves to communicate between intestine and liver to regulate hepatic bile acid synthesis (Fig. 7A). Loss of Diet1 function leads to reduced FGF15 levels, impaired feedback regulation of *Cyp7a1*, and subsequent dysregulated bile acid synthesis (Fig. 7B).

Our conclusion that Diet1 levels in the small intestine influence hepatic bile acid metabolism through effects on FGF15/19 is based on several observations. First, Diet1 deficiency led to reduced *Fgf15* mRNA and protein levels in ileum, and restoration of very low levels of *Diet1* expression by transgenesis caused increased *Fgf15* expression levels in B6By intestine. Furthermore, variations in the level of *Diet1* expression were correlated with intestinal *Fgf15* expression levels, and negatively correlated with hepatic *Cyp7a* expression levels. Second, introduction of FGF15 into Diet1-deficient mice via adenoviral-mediated expression led to a dramatic reduction in *Cyp7a1* mRNA levels, indicating that the lack of FGF15 is a key component of the effects of Diet1 deficiency. Third, acute changes in *Diet1* expression levels in a human intestinal cell line modulated FGF19 production: *Diet1* overexpression increased, and *Diet1* knockdown reduced, the amount of secreted FGF19. And fourth, Diet1 and FGF15/19 proteins showed evidence of a physical interaction. Specifically, Diet1 and FGF15 exhibited an overlapping subcellular distribution in vesicle-like structures, and Diet1 and FGF15/19 proteins co-immunoprecipitated in a complex. Together, these data demonstrate that Diet1 and FGF15/19 are associated both functionally and physically.

A key prediction of our model shown in Fig. 7 is that Diet1-deficient mice should resemble genetically engineered mice with reduced FGF15 levels or enhanced *Cyp7a1* expression. This is indeed the case. Diet1-deficient mice exhibit increased bile acid excretion and elevated hepatic *Cyp7a1* expression, as observed in *Fgf15* knockout mice (Inagaki et al., 2005), and elevated bile acid levels in intestine, gall bladder and feces, and resistance to diet-induced hyperlipidemia, as seen in *Cyp7a1* transgenic mice (Li et al., 2011; Li et al.,

2010). However, in contrast to the increased intestinal *Fgf15* expression that occurs in *Cyp7a1* transgenic mice, Diet1-deficient mice have reduced *Fgf15* mRNA levels, consistent with a role for Diet1 in attaining optimal FGF15 levels. *Fgf15* gene expression is regulated by FXRα, and intestine-specific FXRα deficiency results in reduced *Fgf15* gene expression despite a modestly increased bile acid pool size (Kim et al., 2007). This raises the question of whether Diet1 deficiency reduces *Fgf15* expression via an FXRα-mediated mechanism. Our data suggest that this is not the case, since Diet1-deficient mice express several FXRα target genes at normal levels in liver (*Nr0b2, Abcb11*) and ileum (*Nr0b2, Fabp6, Osta, Ostb*).

Gain- and loss-of-function studies revealed that Diet1 influences FGF15/19 production at both the mRNA and post-transcriptional levels. Diet1-deficient mice had reduced intestinal *Fgf15* mRNA levels, and transient Diet1 overexpression in human HT-29 cells modestly increased endogenous *FGF19* mRNA levels. Additionally, Diet1 expression increased FGF19 protein levels independent of effects on mRNA levels, as demonstrated using FGF19 under the control of a heterologous promoter. This suggests that Diet1 protein may directly influence FGF15/19 protein stability, trafficking or secretion. In support of this possibility, Diet1 and FGF15/19 proteins co-immunoprecipitated and exhibited overlapping subcellular co-localization in a punctate cytosolic pattern. We failed to detect Diet1 co-localization with markers of early endosomal, late endosomal or lysosomal compartments, suggesting that Diet1 may inhabit a specialized endosomal compartment.

Recent studies in humans have shown important relationships between FGF19 levels, bile acid synthetic rates, and intestinal disorders (reviewed in Angelin et al., 2012). It has been known for decades that elevated bile acid levels occur in Crohn's disease, congenital diarrhea, post-infectious diarrhea, short bowel syndrome and disorders classified as idiopathic diarrhea or bile acid malabsorption syndromes (Walters and Pattni, 2010). Recently, it has been proposed that the elevated bile acid levels in many, and perhaps most, of these conditions are not a result of impaired bile acid absorption in the intestine, but rather of increased hepatic bile acid synthesis due to impaired negative feedback regulation (Hofmann, 2009; Johnston et al., 2011; Walters and Pattni, 2010). Walters and colleagues demonstrated a central role for low levels of FGF19 and bile acid diarrhea (Walters et al., 2009). Furthermore, in a study of more than 400 healthy individuals, bile acid synthesis rates (as inferred by measurements of serum 7α-hydroxy-4-cholesten-3-one),were negatively correlated with FGF19 levels (Galman et al., 2011).

The findings described above suggest that inter-individual variations in bile acid levels, as well as pathogenic elevations in bile acid levels observed in disease, may reflect variations in FGF19 levels. Therapeutic strategies that modulate FGF19 levels may be warranted. In the case of chronic bile acid diarrhea syndromes (previously called bile acid malabsorption syndromes), strategies to elevate FGF19 to normal levels would be desirable. On the other hand, individuals with hyperlipidemia may benefit from promoting bile acid synthesis. This has historically been achieved by treatment with bile acid sequestrants, which have recently received attention as a potential means to reduce both hyperlipidemia and hyperglycemia (Aggarwal et al., 2012; Handelsman 2011; Out et al., 2012). Problems remain with bile acid sequestrants, however, in their palatability and long-term adherence rates. The modulation of FGF19 levels up or down thus appears to be an attractive alternative therapeutic strategy for bile acid overproduction syndromes and hyperlipidemia, respectively. Diet1 levels appear to be a control point for FGF15/19 levels. At present, it is unknown what regulates *Diet1* expression; preliminary studies in our laboratory indicate that neither bile acids nor agonists for FXR or several other nuclear receptors have significant effects, and this will require further investigation.

Finally, our findings raise the possibility that common genetic variations in *DIET1* may influence bile acid and lipid levels in the general population, and that rare mutations may underlie conditions characterized by low FGF19 levels, including bile acid malabsorption syndromes. An examination of data from recent genome-wide association studies (Aulchenko et al., 2009; Chasman et al., 2009; Kathiresan et al., 2009; Sandhu et al., 2008; Teslovich et al., 2010) has not revealed genome-wide significant associations between the interval on chromosome 10p12 that harbors the *DIET1* gene and lipid levels in the general population. This is not unexpected, since we predict that genetic variations in *DIET1* should influence lipid levels indirectly through an effect on bile acid synthesis and feedback regulation, and thus would best be detected in individuals with hyperlipidemia in conjunction with low bile acid levels. Thus, a better evaluation of whether common variations in *DIET1* have effects on lipid levels awaits the analysis of a large study sample in which bile acid levels are available. Future studies will also address whether rare mutations in *DIET1* may underlie conditions characterized by high bile acid and low FGF19 levels, as described in some cases of idiopathic bile acid malabsorption (Walters et al., 2009).

EXPERIMENTAL METHODS

Diet1 genetic mapping

C57BL/6ByJ, C57BL/6J, and CAST/EiJ mice were obtained from The Jackson Laboratory (Bar Harbor, ME). Mice were reared and handled according to guidelines established by *The Guide for the Care and Use of Laboratory Animals*, and approved by the UCLA Animal Research Committee. For high-resolution genetic mapping of the *Diet1* gene, C57BL/6ByJ mice were crossed with CAST/EiJ, and the resulting F1 animals were backcrossed to C57BL/6ByJ. At 3 weeks of age, genotype analysis was performed using DNA microsatellite markers that had previously been mapped to the region of interest. At 2 months of age, backcross progeny were fed the atherogenic diet (7.5% cocoa butter, 1.25% cholesterol, 0.5% sodium cholate; TD90221, Teklad Research Diets, Madison, WI) for three weeks. Blood samples were obtained before and at the conclusion of the diet feeding period. Bile acid levels were determined in 50 μl of plasma using an enzymatic assay (Sigma Diagnostics, St. Louis, MO) (Phan et al., 2002). Sequencing of the wild-type and mutant *Diet1* genes was performed as described in the Supplemental Materials.

Diet1 transgenic mice

Diet1 transgenic (*Diet1*-Tg) mice were produced by cloning C57BL/6J mouse *Diet1* cDNA downstream of the regulatory sequences of the rat intestinal fatty acid binding protein (−1178 to +28), which direct expression to small intestine (Cohn et al., 1992), and upstream of a C-terminal V5 epitope tag and an SV40 intron/poly (A) sequence. Microinjection into fertilized mouse C57BL/6J oocytes was performed to establish a transgenic line. Expression of the transgene was distinguished from endogenous *Diet1* using PCR primers that span the Diet1–V5 junction and antibodies directed against V5 (Bethyl Laboratories, Montgomery, TX). To rescue Diet1 expression in B6By mice, transgenic mice were crossed to B6By, and F1 progeny backcrossed to B6By mice. Non-transgenic mice homozygous for the B6By *Diet1* null allele (no endogenous Diet1) were compared with littermates that were homozygous for the B6By *Diet1* allele and hemizygous for the *Diet1*-V5 transgene.

Diet1 expression and knockdown

The coding sequences of human *DIET1* was amplified by PCR without the stop codon, and TA-cloned into the pcDNA3.1-V5/His-TOPO expression vector (Invitrogen) to obtain the V5/His epitope tag in frame with the Diet1 protein. Human intestinal cell line HT-29 was transfected with either empty vector or DIET1-V5 with BioT transfection reagent (Bioland).

Knockdown studies were performed using a pool of three custom Stealth siRNAs (Invitrogen) (CAGCCCAAUCCUUAAUGCCACUGAU; CAGACAGGACCUGGAUGCAUACUUU; GAGUUGCAGAUAGUUACCAAUAGUA) transfected into cells with Lipofectamine RNAiMAX (Invitrogen). As a control, cells were transfected with scrambled siRNA (UCCAACCAGUGGGUGAAACUGUUAA). 48 hr after transfection, culture medium was collected for protein quantitation, and cells were collected for RNA isolation. FGF19 and apolipoprotein AI protein levels were determined in the culture medium using an FGF19 ELISA immunoassay (R & D Systems) and Human Apolipoprotein AI ELISApro (Mabtech), respectively. For studies of Diet1 effects on FGF19 at the post-transcriptional level, FGF19 was expressed under the control of a heterologous promoter in the pcDNA6/Myc-His expression vector (Invitrogen). Levels of cellular Diet1 and FGF19 protein and secreted FGF19 protein were assessed by Western blot analysis and quantified with ImageJ software.

Diet1 subcellular localization in ileum and cultured cells

Ileum was harvested and processed as described in (McConnell et al., 2009) and Supplemental Materials, and frozen sections prepared. Sections were stained with anti-ASBT antibody (a gift of Paul Dawson) and anti-V5 antibody (Bethyl Laboratories), and secondary fluor-conjugated antibodies. Nuclei were stained with DAPI (4',6-diamidino-2-phenylindole). Immunofluorescent images were collected on a Leica TCS SP2 AOBS laser scanning confocal microscope (Mannheim, Germany). Immunofluorescence in the IEC-6 rat intestinal cell line was performed on cells transfected with a mouse Diet1-V5 expression plasmid and an adenovirus expressing Fgf15 (generously provided by Drs. Steve Kliewer and David Mangelsdorf) with antibodies against endogenous EEA1, Rab5, and LimpII as described in Supplemental Materials.

Statistical Analysis

Pairwise comparisons between groups were performed by Student's *t* test unless otherwise indicated in figure legends. Error bars shown throughout represent S.D.

Additional methods

Complete descriptions of *Diet1* sequencing, Southern and Northern blot analyses, *in situ* hybridization, immunohistochemistry and immunofluorescence, co-immunoprecipitation studies, human genetic studies, and PCR primer sequences are provided in Supplemental Materials.

Supplementary Material

Refer to Web version on PubMed Central for supplementary material.

Acknowledgments

We thank Dr. Peter Edwards for helpful discussions, Dr. Paul Dawson for the ASBT antibody, Drs. Steven Kliewer and David Mangelsdorf for FGF15 adenovirus, and Ping Xu for technical assistance. KR was supported by grants from the National Institutes of Health (HL58627, HL28481 and HL102661) and the Veterans Administration (Merit Award). JML was supported by NIH training grant GM007104-34. JA was supported by grants from the European Research Council, Swiss National Science Foundation, and the EPFL.

REFERENCES

Aggarwal S, Loomba RS, Arora RR. Efficacy of colesevelam on lowering glycemia and lipids. J. Cardiovasc. Pharmacol. 2012; 59:198–205. [PubMed: 21983746]

Allen K, Gokay KE, Thomas MA, Speelman BA, Wilson JM. Biosynthesis of endotubin: an apical early endosomal glycoprotein from developing rat intestinal epithelial cells. Biochem. J. 1998; 330:367–373. [PubMed: 9461532]

Angelin B, Eriksson M, Rudling M. Bile acids and lipoprotein metabolism: a renaissance for bile acids in the post-statin era? Curr. Opin. Lipidol. 1999; 10:269–274. [PubMed: 10431663]

Angelin B, Larsson TE, Rudling M. Circulating fibroblast growth factors as metabolic regulators—a critical appraisal. Cell Metab. 2012; 16:693–705. [PubMed: 23217254]

Aulchenko YS, Ripatti S, Lindqvist I, Boomsma D, Heid IM, Pramstaller PP, Penninx BW, Janssens AC, Wilson JF, Spector T, et al. Loci influencing lipid levels and coronary heart disease risk in 16 European population cohorts. Nat. Genet. 2009; 41:47–55. [PubMed: 19060911]

Beckmann G, Bork P. An adhesive domain detected in functionally diverse receptors. Trends. Biochem. Sci. 1993; 18:40–41. [PubMed: 8387703]

Chasman DI, Pare G, Mora S, Hopewell JC, Peloso G, Clarke R, Cupples LA, Hamsten A, Kathiresan S, Malarstig A, Ordovas JM, Ripatti S, Parker AN, Miletich JP, Ridker PM. Forty-three loci associated with plasma lipoprotein size, concentration, and cholesterol content in genome-wide analysis. PLoS Genet. 2009; 5:e1000730. [PubMed: 19936222]

Cicione C, Degirolamo C, Moschetta A. Emerging role of fibroblast growth factors 15/19 and 21 as metabolic integrators in the liver. Hepatology. 2012; 56:2404–2411. [PubMed: 22753116]

Cismasiu VB, Denes SA, Reilander H, Michel H, Szedlacsek SE. The MAM (meprin/A5-protein/PTPmu) domain is a homophilic binding site promoting the lateral dimerization of receptor-like protein-tyrosine phosphatase mu. J. Biol. Chem. 2004; 279:26922–26931. [PubMed: 15084579]

Cohn SM, Simon TC, Roth KA, Birkenmeier EH, Gordon JI. Use of transgenic mice to map cis-acting elements in the intestinal fatty acid binding protein gene (Fabpi) that control its cell lineage-specific and regional patterns of expression along the duodenal-colonic and crypt-villus axes of the gut epithelium. J. Cell Biol. 1992; 119:27–44. [PubMed: 1527171]

Dawson PA, Lan T, Rao A. Bile acid transporters. J. Lipid Res. 2009; 50:2340–2357. [PubMed: 19498215]

Galman C, Angelin B, Rudling M. Pronounced variation in bile acid synthesis in humans is related to gender, hypertriglyceridaemia and circulating levels of fibroblast growth factor 19. J. Int. Med. 2011; 270:580–588.

Gokay KE, Young RS, Wilson JM. Cytoplasmic signals mediate apical early endosomal targeting of endotubin in MDCK cells. Traffic. 2001; 2:487–500. [PubMed: 11422942]

Goldfine AB. Modulating LDL cholesterol and glucose in patients with type 2 diabetes mellitus: targeting the bile acid pathway. Curr. Opin. Cardiol. 2008; 23:502–511. [PubMed: 18670263]

Hageman J, Herrema H, Groen AK, Kuipers F. A role of the bile salt receptor FXR in atherosclerosis. Arterioscler. Thromb. Vasc. Biol. 2010; 30:1519–1528. [PubMed: 20631352]

Handelsman Y. Role of bile acid sequestrants in the treatment of type 2 diabetes. Diabetes Care 34. 2011; 2(Suppl.):S244–S250.

Hofmann AF. The enterohepatic circulation of bile acids in mammals: form and functions. Front. Biosci. 2009; 14:2584–2598.

Hylemon PB, Zhou H, Pandak WM, Ren S, Gil G, Dent P. Bile acids as regulatory molecules. J. Lipid Res. 2009; 50:1509–1520. [PubMed: 19346331]

Inagaki T, Choi M, Moschetta A, Peng L, Cummins CL, McDonald JG, Luo G, Jones SA, Goodwin B, Richardson JA, Gerard RD, Repa JJ, Mangelsdorf DJ, Kliewer SA. Fibroblast growth factor 15 functions as an enterohepatic signal to regulate bile acid homeostasis. Cell Metab. 2005; 2:217–225. [PubMed: 16213224]

Ishmael FT, Shier VK, Ishmael SS, Bond JS. Intersubunit and domain interactions of the meprin B metalloproteinase. Disulfide bonds and protein-protein interactions in the MAM and TRAF domains. J. Biol. Chem. 2005; 280:13895–13901. [PubMed: 15695509]

Johnston I, Nolan J, Pattni SS, Walters JR. New insights into bile acid malabsorption. Curr. Gastroenterol. Rep. 2011; 13:418–425. [PubMed: 21805078]

Jones SA. Mini-review: endocrine actions of fibroblast growth factor 19. Mol. Pharm. 2008; 5:42–48. [PubMed: 18179175]

Jones SA. Physiology of FGF15/19. Adv. Exp. Med. Biol. 2012; 728:171–182. [PubMed: 22396169]

Kathiresan S, Willer CJ, Peloso GM, Demissie S, Musunuru K, Schadt EE, Kaplan L, Bennett D, Li Y, Tanaka T, et al. Common variants at 30 loci contribute to polygenic dyslipidemia. Nat. Genet. 2009; 41:56–65. [PubMed: 19060906]

Khurana S, Raufman JP, Pallone TL. Bile acids regulate cardiovascular function. Clin. Transl. Sci. 2011; 4:210–218. [PubMed: 21707953]

Kim I, Ahn SH, Inagaki T, Choi M, Ito S, Guo GL, Kliewer SA, Gonzalez FJ. Differential regulation of bile acid homeostasis by the farnesoid X receptor in liver and intestine. J. Lipid Res. 2007; 48:2664–2672. [PubMed: 17720959]

Lefebvre P, Cariou B, Lien F, Kuipers F, Staels B. Role of bile acids and bile acid receptors in metabolic regulation. Physiol. Rev. 2009; 89:147–191. [PubMed: 19126757]

Li T, Matozel M, Boehme S, Kong B, Nilsson LM, Guo G, Ellis E, Chiang JY. Overexpression of cholesterol 7alpha-hydroxylase promotes hepatic bile acid synthesis and secretion and maintains cholesterol homeostasis. Hepatology. 2011; 53:996–1006. [PubMed: 21319191]

Li T, Owsley E, Matozel M, Hsu P, Novak CM, Chiang JY. Transgenic expression of cholesterol 7alpha-hydroxylase in the liver prevents high-fat diet-induced obesity and insulin resistance in mice. Hepatology. 2010; 52:678–690. [PubMed: 20623580]

Lundasen T, Galman C, Angelin B, Rudling M. Circulating intestinal fibroblast growth factor 19 has a pronounced diurnal variation and modulates hepatic bile acid synthesis in man. J. Int. Med. 2006; 260:530–536.

McCarter SD, Johnson DL, Kitt KN, Donohue C, Adams A, Wilson JM. Regulation of tight junction assembly and epithelial polarity by a resident protein of apical endosomes. Traffic. 2010; 11:856–866. [PubMed: 20214753]

McConnell RE, Higginbotham JN, Shifrin DA Jr, Tabb DL, Coffey J, Tyska MJ. The enterocyte microvillus is a vesicle-generating organelle. J. Cell Ciol. 2009; 185:1285–1298.

Mouzeyan A, Choi J, Allayee H, Wang X, Sinsheimer J, Phan J, Castellani LW, Reue K, Lusis AJ, Davis RC. A locus conferring resistance to diet-induced hypercholesterolemia and atherosclerosis on mouse chromosome 2. J. Lipid Res. 2000; 41:573–582. [PubMed: 10744778]

Out C, Groen AK, Brufau G. Bile acid sequestrants: more than simple resins. Curr. Opin. Lipidol. 2012; 23:45–53.

Phan J, Pesaran T, Davis RC, Reue K. The Diet1 locus confers protection against hypercholesterolemia through enhanced bile acid metabolism. J. Biol. Chem. 2002; 277:469–477. [PubMed: 11682476]

Potthoff MJ, Boney-Montoya J, Choi M, He T, Sunny NE, Satapati S, Suino-Powell K, Xu HE, Gerard RD, Finck BN, Burgess SC, Mangelsdorf DJ, Kliewer SA. FGF15/19 regulates hepatic glucose metabolism by inhibiting the CREB-PGC-1alpha pathway. Cell Metab. 2011; 13:729–738. [PubMed: 21641554]

Quaroni A, Wands J, Trelstad RL, Isselbacher KJ. Epithelioid cell cultures from rat small intestine. Characterization by morphologic and immunologic criteria. J. Cell Biol. 1979; 80:248–265. [PubMed: 88453]

Rousset M, Laburthe M, Pinto M, Chevalier G, Rouyer-Fessard C, Dussaulx E, Trugnan G, Boige N, Brun JL, Zweibaum A. Enterocytic differentiation and glucose utilizatio in the human colon trumor cell line Caco-2: modulation by forskolin. J. Cell. Physiol. 1985; 123:377–385. [PubMed: 2985631]

Russell DW. The enzymes, regulation, and genetics of bile acid synthesis. Annu. Rev. Biochem. 2003; 72:137–174. [PubMed: 12543708]

Russell DW. Fifty years of advances in bile acid synthesis and metabolism. J. Lipid Res. 2009; 50:S120–S125. [PubMed: 18815433]

Sandhu MS, Waterworth DM, Debenham SL, Wheeler E, Papadakis K, Zhao JH, Song K, Yuan X, Johnson T, Ashford S, et al. LDL-cholesterol concentrations: a genome-wide association study. Lancet. 2008; 371:483–491. [PubMed: 18262040]

Schmidt DR, Holmstrom SR, Fon Tacer K, Bookout AL, Kliewer SA, Mangelsdorf DJ. Regulation of bile acid synthesis by fat-soluble vitamins A and D. J. Biol. Chem. 2010; 285:14486–14494. [PubMed: 20233723]

Semple TU, Quinn LA, Woods LK, Moore GE. Tumor and lymphoid cell lines from a patient with carcinoma of the colon for a cytotoxicity model. Cancer Res. 1978; 38:1345–1355. [PubMed: 565251]

Teslovich TM, Musunuru K, Smith AV, Edmondson AC, Stylianou IM, Koseki M, Pirruccello JP, Ripatti S, Chasman DI, Willer CJ, et al. Biological, clinical and population relevance of 95 loci for blood lipids. Nature. 2010; 466:707–713. [PubMed: 20686565]

Thomas C, Pellicciari R, Pruzanski M, Auwerx J, Schoonjans K. Targeting bile-acid signalling for metabolic diseases. Nat. Rev. Drug Discov. 2008; 7:678–693. [PubMed: 18670431]

Walters JR, Pattni SS. Managing bile acid diarrhoea. Therap. Adv. Gastroenterol. 2010; 3:349–357.

Walters JR, Tasleem AM, Omer OS, Brydon WG, Dew T, le Roux CW. A new mechanism for bile acid diarrhea: defective feedback inhibition of bile acid biosynthesis. Clin. Gastroenterol. Hepatol. 2009; 7:1189–1194. [PubMed: 19426836]

Westergaard H. Bile Acid malabsorption. Curr. Treat. Options Gastroenterol. 2007; 10:28–33. [PubMed: 17298762]

Wilson JM, Colton TL. Targeting of an intestinal apical endosomal protein to endosomes in nonpolarized cells. J. Cell Biol. 1997; 136:319–330. [PubMed: 9015303]

Wright TJ, Ladher R, McWhirter J, Murre C, Schoenwolf GC, Mansour SL. Mouse FGF15 is the ortholog of human and chick FGF19, but is not uniquely required for otic induction. Dev. Biol. 2004; 269:264–275. [PubMed: 15081372]

Yamamoto T, Ryan RO. Domain Swapping Reveals That Low Density Lipoprotein (LDL) Type A Repeat Order Affects Ligand Binding to the LDL Receptor. J. Biol. Chem. 2009; 284:13396–13400. [PubMed: 19329437]

Zweibaum A, Triadou N, Kedinger M, Augeron C, Robine-Leon S, Pinto M, Rousset M, Haffen K. Sucrase-isomaltase: a marker of foetal and malignant epithelial cells of the human colon. Int. J. Cancer. 1983; 32:407–412. [PubMed: 6352518]

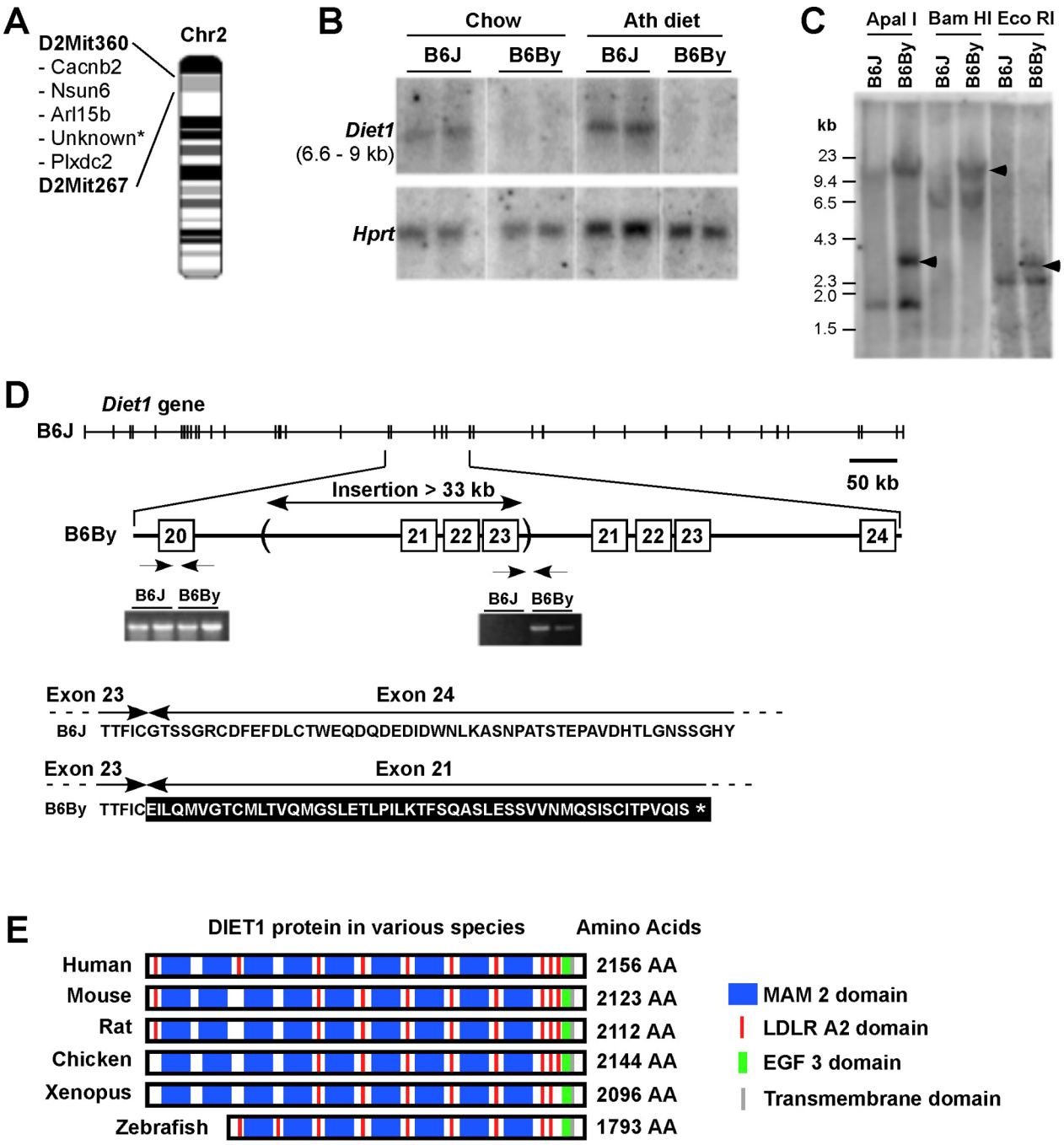

Figure 1. Identification of the *Diet1* gene mutation in C57BL/6ByJ mice by positional cloning

(A) Localization of the *Diet1* gene on mouse chromosome 2 by mapping in a C57BL/6ByJ (B6By) × CAST/EiJ backcross. The delimiting DNA microsatellite markers and known genes in the interval are listed. The gene labeled “Unknown” was a collection of several predicted genes that we determined by sequencing to belong to a single *Diet1* mRNA transcript.

(B) Northern blots showing *Diet1* mRNA expression in small intestine of C57BL/6J (B6J) but not B6By mice. *Diet1* expression levels are similar in C57BL/6J mice fed chow and

atherogenic (Ath) diets after normalization to hypoxanthine phosphoribosyltransferase (Hprt). *Diet1* mRNA migrates between RNA ladder markers sized 6.6–9 kb.
(C) Southern blot of B6J and B6By genomic DNA probed with exon 23 of the *Diet1* gene. Duplication of part of the gene is evident as extra bands detectable in B6By samples (arrows) upon digestion with *ApaLI*, *BamHI*, and *EcoRI*.
(D) *Top*, Genomic structure of the wild-type mouse *Diet1* gene. Vertical bars represent exons. *Middle*, Duplication of exons 21–23 in the B6By mutant allele. Sequence analysis positioned the duplicated region 15 kb downstream of exon 20. The inset illustrates detection exclusively in B6By mice of a PCR product generated with primers spanning the 3' boundary of the duplicated region (primers mDiet1dup, Supplemental Experimental Procedures). *Lower*, Black shading indicates the altered amino acid sequence and premature stop codon (denoted by asterisk) that result from mutation in B6By mice. The normal sequence in C57BL/6J mice is shown above for comparison.
(E) Schematic structure and predicted functional motifs in Diet1 protein from the species indicated; the predicted number of amino acids is shown at right. Functional domains were predicted by Prosite. MAM, meprin–A5–protein tyrosine phosphatase mu; LDLR A2, low density lipoprotein receptor A2 motif; EGF, epidermal growth factor. The gray bar represents a predicted transmembrane domain.

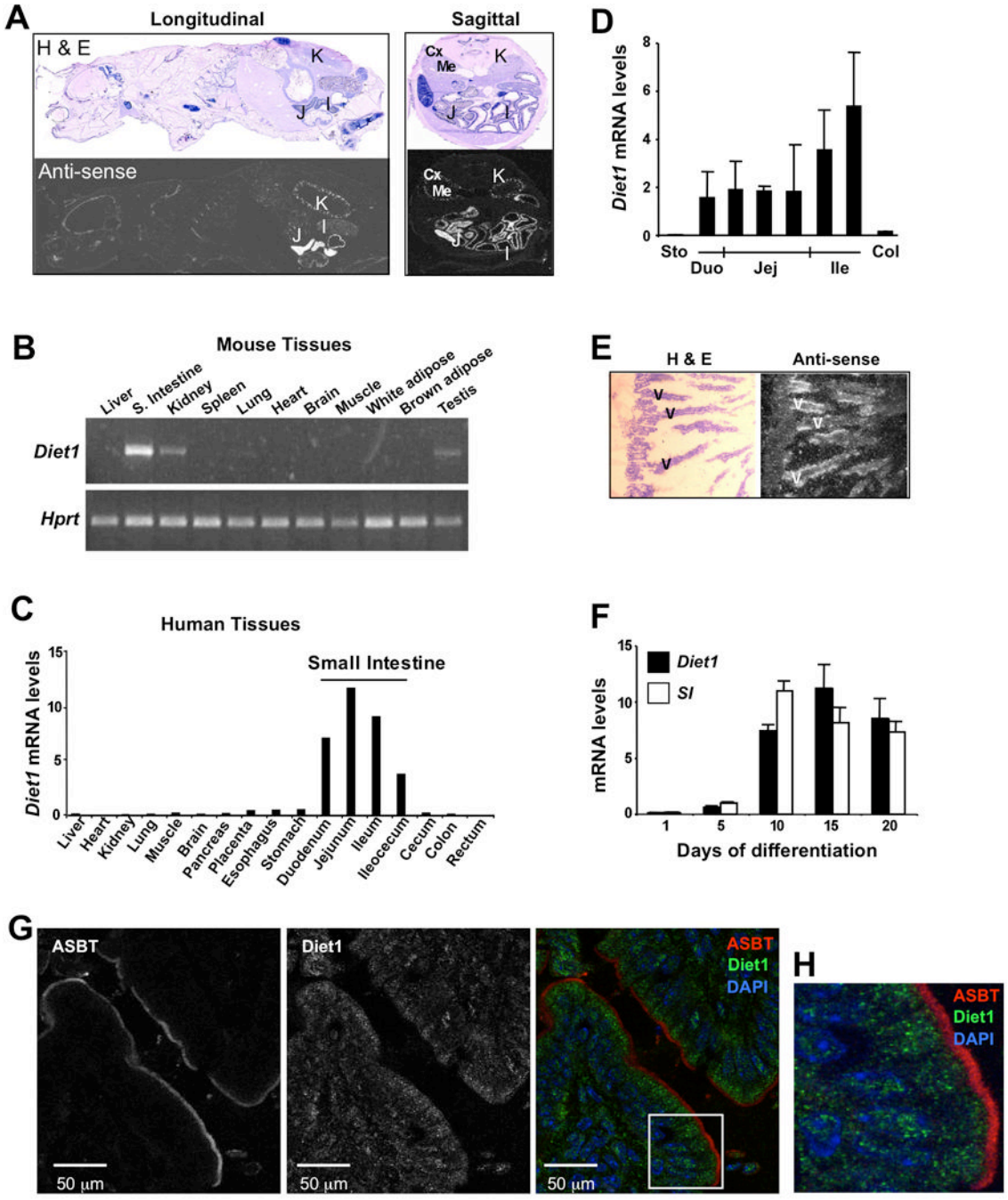

Figure 2. *Diet1* expression in enterocytes of the small intestine

(A) *In situ* RNA hybridization analysis of *Diet1* expression in adult whole mouse sections. *In situ* hybridization was performed on whole mouse longitudinal or sagittal sections using a *Diet1* complementary RNA probe. Images at the top show sections stained with hematoxylin and eosin and images at the bottom show the *in situ* hybridization signals. J, jejunum; I, Ileum; K, kidney; Cx, renal cortex; Me, renal medulla.

(B) *Diet1* mRNA expression in a mouse tissue panel determined by RT-PCR. Corresponding *Hprt* expression levels are shown. S. Intestine, small intestine.

(C) *DIET1* mRNA expression in pooled human tissue samples. *DIET1* mRNA was quantitated by qPCR and normalized to *HPRT* and β2-microglobulin expression.
(D) qPCR quantitation of *Diet1* mRNA expression levels in mouse gastrointestinal tract. N = 3 (mean ± SD). Sto, stomach; Duo, duodenum; Jej, jejunum; Ile, ileum; Col, colon.
(E) High resolution *in situ* image from small intestine shows *Diet1* mRNA (light granules) concentrated in epithelial cells along the surface of villi (V).
(F) Induction of endogenous *DIET1* mRNA expression during differentiation of the Caco-2 human intestinal cell line. The expression of sucrase isomaltase (SI) is shown as a positive control for differentiation. All measurements were determined by qPCR and normalized against *HPRT* and β2-microglobulin expression. N = 3 (mean ± SD).
(G) Diet1 protein visualized in mouse intestinal enterocytes by immunofluorescent confocal microscopy. Intestine from a mouse strain expressing a V5-epitope tagged Diet1 transgene was stained with antibodies against Diet1-V5 (green). The apical membrane was detected with antibody against the apical salt-dependent bile acid transporter (ASBT, red), and nuclei were stained with DAPI (blue).
(H) Enlargement of boxed region in (G) shows complete lack of co-localization between Diet1 and ASBT.

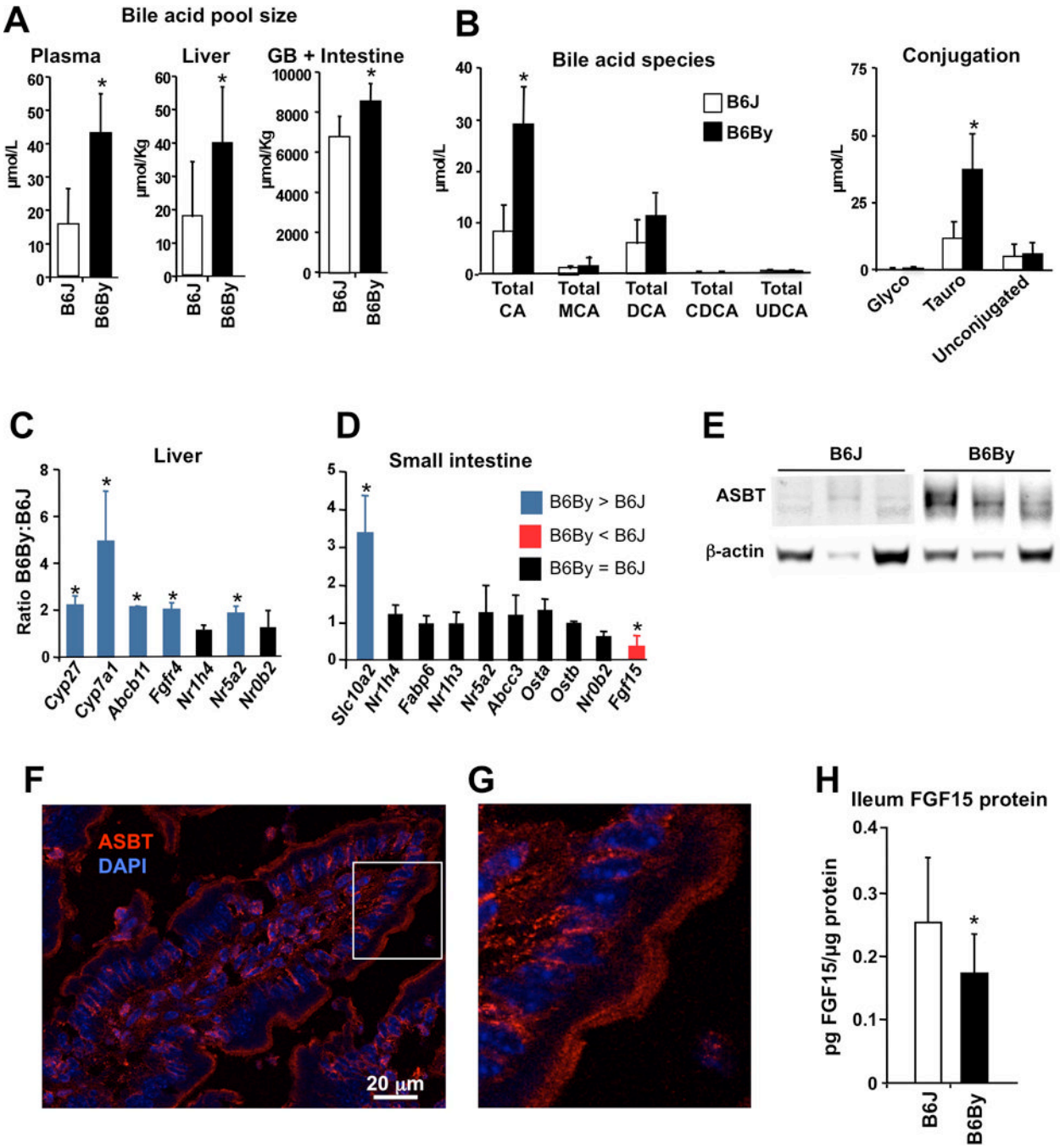

Figure 3. Diet1-deficient mice have increased bile acid pool size and reduced ileal FGF15 mRNA and protein levels

(A) Bile acid content is increased in plasma, liver, and gall bladder (GB) + small intestine of Diet1-deficient B6By compared to B6J mice. After 3 weeks on an atherogenic diet, mice were fasted 16 hr, tissues collected, and bile acid concentrations determined by high performance liquid chromatography followed by enzymatic reaction and fluorescence detection. N = 6 (mean ± SD). *, $p < 0.05$.

(B) Bile acid composition in plasma of B6J and B6By mice from (A). Left, concentration of bile acid species; right, conjugation status of bile acids. CA, cholic acid; MCA, muricholic

acid; DCA, deoxycholic acid, CDCA, chenodeoxycholic acid; UDCA, ursodeoxycholic acid. *, $p < 0.05$.

(C, D) Relative gene expression levels in liver (C) and small intestine (D) of B6J and B6By mice determined by qPCR. Values are expressed as the ratio of levels in B6By compared to B6J mice; error bars indicate SD. Black bars indicate genes with similar expression levels in B6By and B6J. Blue bars indicate genes with elevated expression in B6By mice, and the red bar indicates the gene with reduced expression in B6By mice compared to B6J mice. See text for full gene names. *, $p < 0.05$ in B6By *versus* B6J.

(E) Western blot analysis of ASBT in ileum of B6J and B6By mice. β-actin is shown as a loading control from a different region of the same gel lanes.

(F) ASBT protein visualized in B6By mouse intestinal enterocytes via immunofluorescent confocal microscopy. ASBT is in red, and DNA is stained blue with DAPI.

(G) Enlarged inset from panel (F).

(H) FGF15 protein quantification (mean ±SD) in B6J and B6By mouse ileum by ELISA. Validation of the specificity of this ELISA is shown in Figure S5. *, $p < 0.05$.

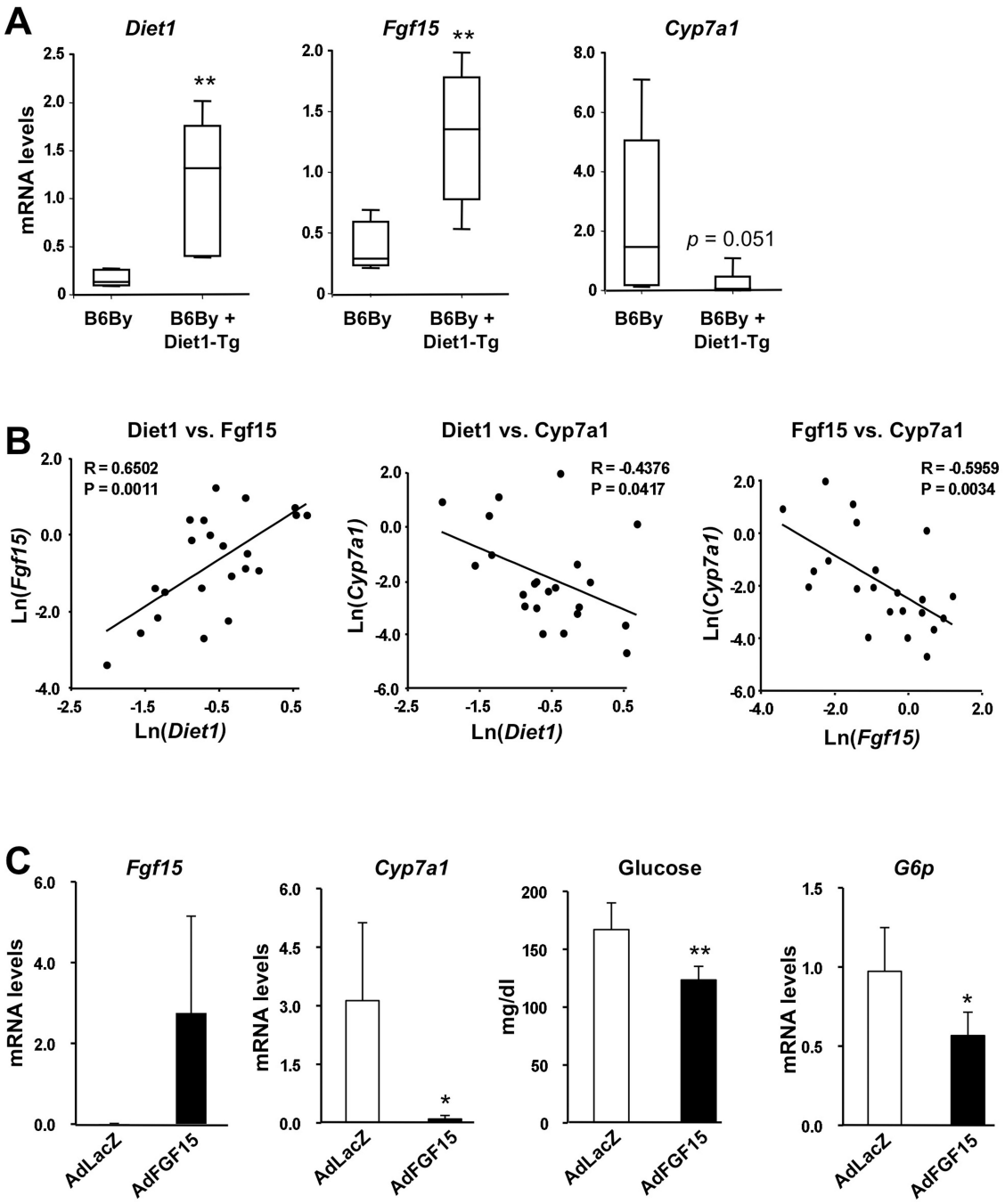

Figure 4. *In vivo* correlation between *Diet1*, *Fgf15* and *Cyp7a1* expression, and *Cyp7a1* normalization by adenovirus-mediated Fgf15 expression in Diet1-deficient mice

(A) qPCR analysis of intestinal *Diet1* and *Fgf15*, and hepatic *Cyp7a1* mRNA levels in female B6By and B6By+Diet1-Tg mice. Box-and-whisker plots with medians, quartiles (boxes) and minima and maxima (lines) indicated. N = 5 (B6By), 6 (B6By+Diet1-Tg); error bars indicate SD. Statistical significance determined by Mann-Whitney U-Test. **, $p < 0.01$

(B) Correlations between intestinal *Diet1*, intestinal *Fgf15*, and hepatic *Cyp7a1* mRNA levels in individual B6By and B6By+Diet1 Tg mice. Log-transformed (Ln) mRNA levels were used. N = 24.

(C) Adenoviral-mediated expression of FGF15 in Diet1-deficient mice for 6 days *Cyp7a1* mRNA, fasting glucose, and glucose-6-phosphatase (G6p) mRNA levels, all shown as mean ± SD. *, $p < 0.05$ vs. adenoviral-mediated lacZ (AdLacZ) expression.

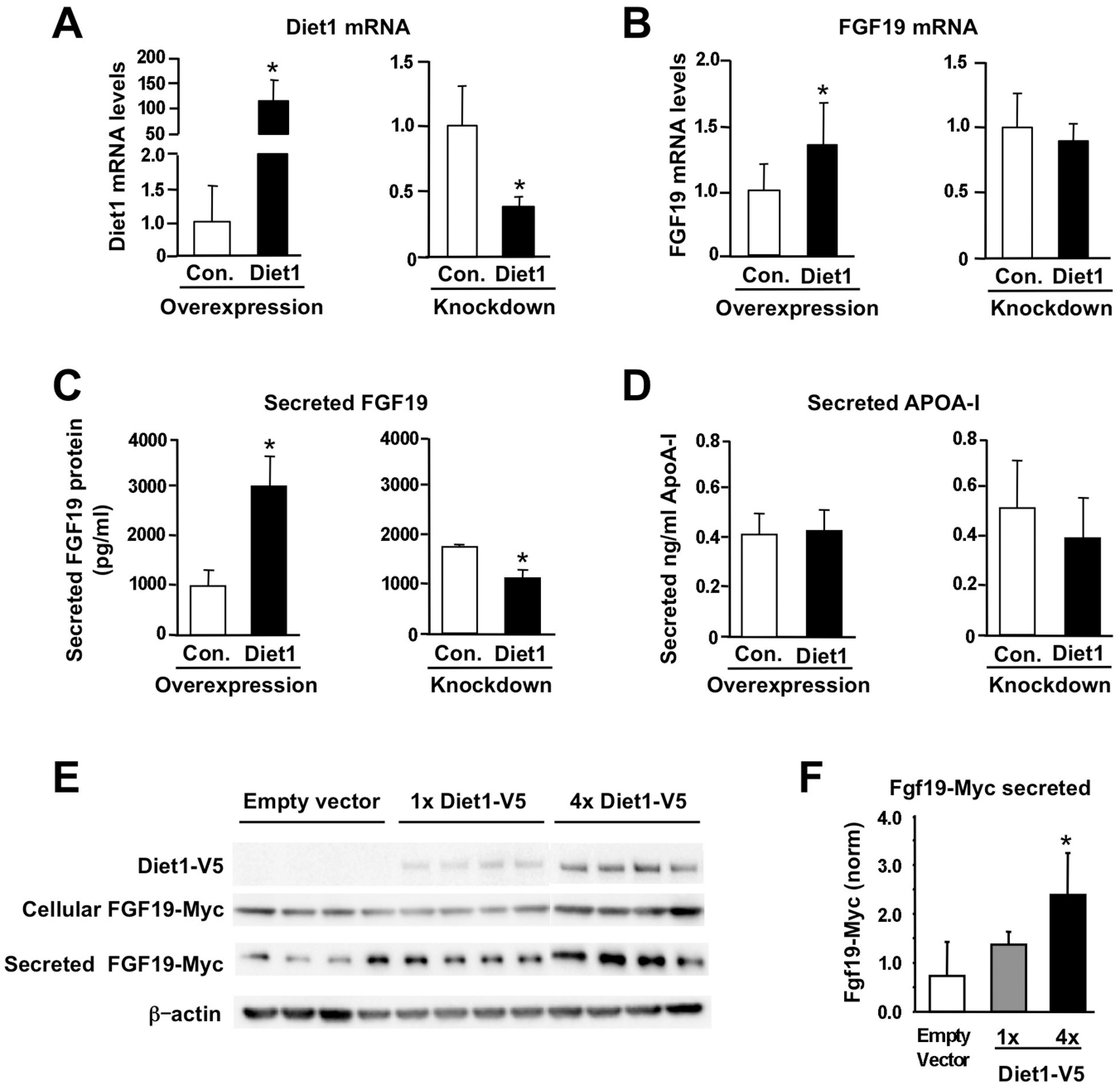

Figure 5. Diet1 levels influence FGF19 production at both the mRNA and post-transcriptional levels

(A) Human *DIET1* expression levels in the human HT-29 intestinal cell line were increased several-fold by transfection with human *DIET1* cDNA (left), or reduced 60% by knockdown with *DIET1* siRNA (right). Levels of expression were compared to control cells (Con.) treated with empty plasmid vector or scrambled siRNA for overexpression and knockdown experiments, respectively. Values represent mean ± SD.

(B) FGF19 mRNA levels from cells in panel (A). *DIET1* overexpression modestly increased FGF19 mRNA, whereas *DIET1* knockdown did not alter *FGF19* expression.

(C) FGF19 protein secreted into the medium of cells in panel (A). FGF19 protein levels increased 3-fold with *DIET1* overexpression, and decreased 40% with partial *DIET1* knockdown.
(D) ApoAI protein secreted into the culture medium of cells cells in panel (A). Levels were unaltered by *DIET1* overexpression or knockdown. Values shown represent mean ± SD for 3 replicates. *, $p < 0.05$ in controls *vs*. overexpression or knockdown samples.
(E) Diet1 influences FGF19 protein levels, in part, at the post-transcriptional level. FGF19 was expressed under control of a heterologous promoter in the absence of Diet1 (empty vector control) or presence of increasing amounts (1× and 4×) of Diet1 expression vector. Cellular and secreted proteins were detected by Western blot. β-actin protein levels were unaffected by Diet1, whereas FGF19 protein increased with higher levels of Diet1.
(F) Quantification of FGF19 from western blot shown in (E) normalized to β-actin. *, $p < 0.05$ *vs*. empty vector control.

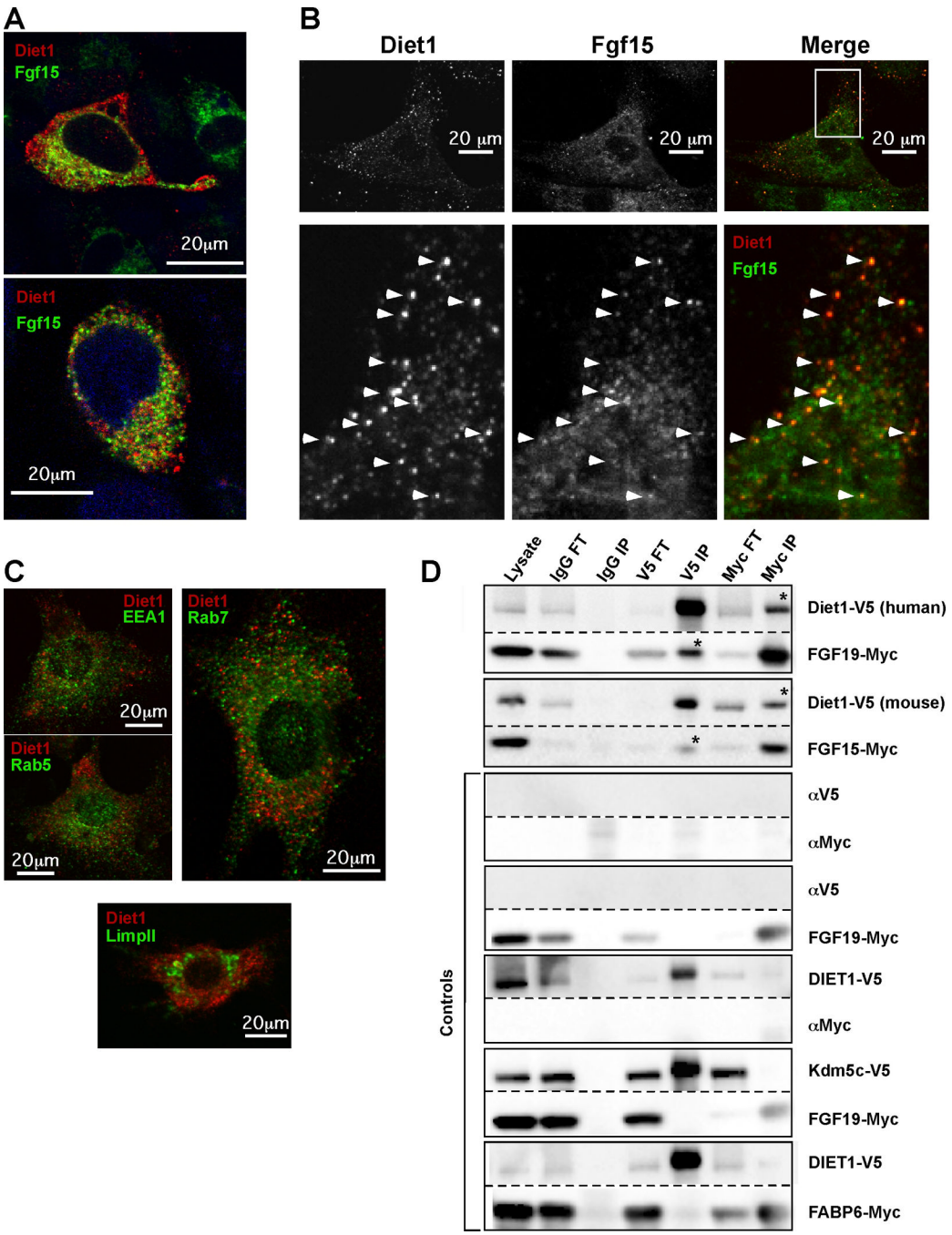

Figure 6. Diet1 and FGF15/FGF19 proteins interact

(A) Subcellular localization of Diet1 and FGF15 proteins overlap in rat intestinal cells. Immunofluorescent confocal microscopy was performed on IEC-6 rat intestinal cells expressing V5-tagged Diet1 and untagged mouse FGF15.

(B) Higher magnification of an IEC-6 cell stained for Diet1 and FGf15 proteins. Several sites of Diet1 and FGF15 co-localization were observed (white arrowheads), which can be appreciated by comparison of single channel black-and-white images to visualize dots with common positions, and by merging images (right panel).

(C) Diet1 failed to co-localize with markers of early endosomes (EEA1, Rab5), late endosomes (Rab7), or lysosomes (LimpII) in IEC-6 cells.

(D) Co-immunoprecipitation of Diet1 and FGF15/FGF19. Human HEK-293T cells were co-transfected with either human Diet1-V5 and FGF19-Myc, mouse Diet1-V5 and FGF15-Myc, or controls including empty vectors and vectors expressing irrelevant proteins (Kdm5c-V5 and FABP6-Myc). Interaction was observed only when human Diet1 and FGF19, or mouse Diet1 and FGF15, were co-transfected (indicated by "*"s in top panels). The interaction occurred in both directions, *e.g.*, when Diet1 was pulled down with the V5 antibody and when FGF19/FGF15 was pulled down with the Myc antibody. Diet1 and FGF19 did not co-immunoprecipitate with irrelevant proteins (Fabp6 or Kdm5c) carrying the V5 and Myc epitope tags.

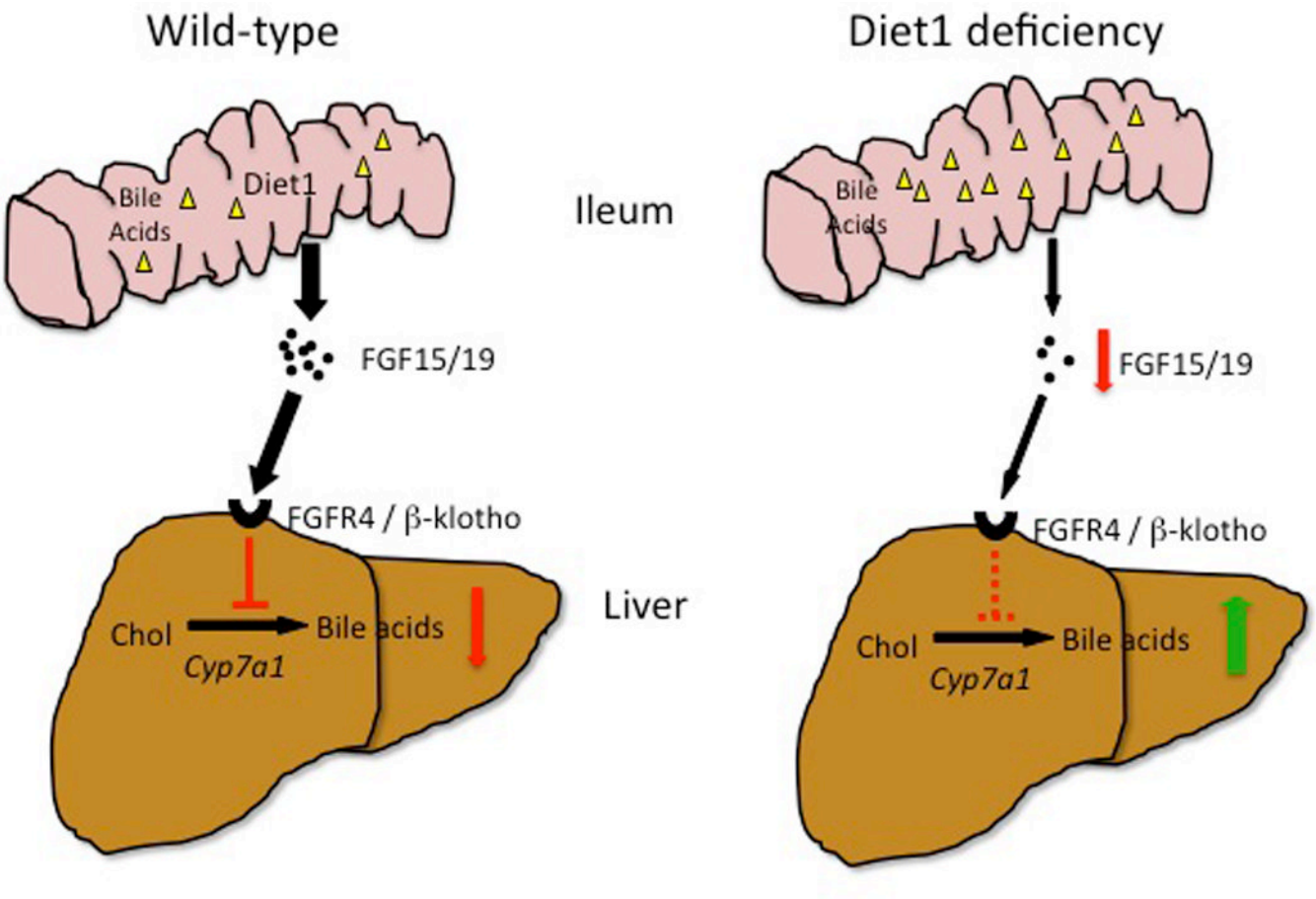

Figure 7. Proposed role of Diet1 in enterohepatic signaling for regulation of bile acid homeostasis

In wild-type animals, Diet1 levels in the small intestine are correlated with levels of FGF15 in ileum, which influence feedback regulation of hepatic *Cyp7a1* expression and resulting bile acid levels. In Diet1-deficient mice, FGF15 levels are diminished and feedback regulation of hepatic bile acid synthesis is impaired, leading to increased bile acid levels in the gastrointestinal tract and circulation.